**Original Study** **Open Access**

Jakub Rainer*, Hubert Szabowicz

# Analysis of underground stratification based on CPTu profiles using high-pass spatial filter

https://doi.org/10.2478/sgem-2020-0002
received February 28, 2020; accepted August 3, 2020.

**Abstract:** The issue of the stratification of the underground subsoil is one of the principal geotechnical challenges. The development of the Cone Penetration Tests (CPTu) has resulted in the possibility to record parameters in a quasi-continuous way, which provides a very detailed description of the soil response. Such accurate measurements may therefore be treated as a signal or image and be analysed as such. This paper presents the application of high-pass spatial filters to perform soil stratification on the basis of the static penetration test. The presented algorithm has been tested on the test data set provided by the Organizers of TC304 Student Contest on Spatial Data Analysis (September 22, 2019, Hannover, Germany). It provides reasonable results at negligible computational cost and is applicable to most soils, especially if the contrast between the parameters of the adjacent layers is significant.

**Keywords:** Cone Penetration Test (CPTu); soil stratification; convolutional filter; high-pass spatial filter.

## 1 Introduction

In recent years it has been popular to incorporate the knowledge of the signal theory into the analysis of CPTu sounding. This paper provides one of the possible ways to perform the ground stratification based on the CPTu sounding using high-pass spatial filters, which are successfully used in the image analysis to detect sudden changes in the intensity of values on the image, that is, the edges.

The study consists of the three main sections. In the beginning, a definition of the edge, basic information on CPTu static sounding and high-pass spatial filters are presented. Further, the author's algorithm is introduced and an example of stratification performed with its use is presented. Finally, the analysis of its operation based on the test data set provided by the Organizers of TC304 Student Contest on Spatial Data Analysis (September 22, 2019, Hannover, Germany) is discussed. The conclusions are presented and the further direction of the algorithm development is outlined.

### 1.1 General characteristic of the Cone Penetration Test

One of the main in situ testing method used in geotechnics to designate the properties of the soil is Cone Penetration Test (CPTu). The popularity of this method is ensured by the simplicity and rapidity of the testing.[7] The measurements recorded during the penetration tests is commonly used to recognize the underground stratification.

The Cone Penetration Test involves pushing a penetration rod finished with a special measurement cone into the ground. The penetration velocity is controlled and should be constant at 20 mm/s. The information from the test cone are sent to the computer at fixed time intervals. Currently, it is possible to probe even 2 times per second, which corresponds to registration in profile every 10 mm. Such frequent sampling may be considered as quasi-constant. During the test, the resistance under the cone tip $q_c$ and local skin friction on the sleeve $f_s$ are registered. Additionally to classical CPT, the CPTu cone is equipped with the pore pressure measurement, which offer the possibility for measuring it at three different locations along the shaft: $u_1$, $u_2$, $u_3$.[7] Because of the geometrical features of the cone (e.g., grooves in the places where filters occur) the registration is disturbed by atmospheric pressure and pore pressure. In order to get rid of them on the values of $q_c$ and $f_s$ recorded during the measurement, it is necessary to switch to standard values by introducing appropriate corrections taking into account additional geometrical parameters.[7] The standardized resistance under the cone is marked as $Q_{tn}$ and the friction on the sleeve as $F_r$ – calculated according to formulas (1) to (6).

***Corresponding author: Jakub Rainer,** Wrocław University of Science and Technology, Wrocław, Poland, E-mail: jakub.rainer@pwr.edu.pl
**Hubert Szabowicz,** Wrocław University of Science and Technology, Wrocław, Poland

$$Q_{tn} = \frac{q_t - \sigma_{v0}}{P_a} \cdot C_N \quad (1)$$

$$F_r(\%) = 100 \cdot \frac{f_s}{q_t - \sigma_{v0}} \quad (2)$$

$$q_t = q_c + u_2 \cdot (1 - a) \quad (3)$$

$$C_N = \left(\frac{P_a}{\sigma'_{v0}}\right)^n \quad (4)$$

$$n = 0.381 \cdot I_c + 0.05 \cdot \frac{P_a}{\sigma'_{v0}} \quad (5)$$

$$I_c = \sqrt{(3.47 - \log Q_{tn})^2 + (\log F_r + 1.22)^2} \quad (6)$$

where $P_a$ – atmospheric pressure, $\sigma'_{v0}$ and $\sigma_{v0}$, respectively – the effective and total overburden stress values, $C_N$ – the correction factor for the effective overburden stress, $n$ – stress exponent determined by the Soil Behaviour Type (SBTn) index $I_c$, $q_t$ – corrected tip resistance, $a$ – net ratio of the tip.[10] All parameters are calculated in an iterative way.

A highly significant parameter necessary in various interpretations is the friction ratio $R_f$,[7] which determines the ratio of sleeve friction to resistance under the cone tip and the standardized pore pressure parameter $B_q$,[8] which is expressed as the ratio of the increase in ground water pore pressure to the difference in resistance under the cone tip, taking into account the effect of ground water pore pressure and primary stress.

$$R_f(\%) = \frac{f_s}{q_t} \cdot 100 \quad (7)$$

$$B_q = \frac{u_2 - u_0}{q_t - \sigma_{v0}} \quad (8)$$

## 1.2 Soil behaviour type classification

During the whole process of ground investigation using a CPTu, sounding a crucial element is the properly performed interpretation of the measurement values obtained from the test. Even the best results may be lost significantly if the interpretation is incorrect. One of the basic applications of the CPTu test is the soil behaviour type classification based on normalized measurement parameters. There are a series of nomograms that allow to identify the soil in the profile. One of the most basic and widely used in the world is the 1986 Robertson classification.[7]

It is based on the relationship between the corrected resistance under the cone tip $q_t$ and the friction ratio $R_f$. The chart area has been divided into 12 Soil Behaviour Types (SBT) areas (Figure 1). Depending on the subdivision in which the measurement point will be located, it is qualified to a given SBT group. The Soil Behaviour Types are defined in Table 1.

**Table 1:** Numbers of subdivisions and corresponding Soil Behaviour Types[7]

| SBT | Soil Behaviour Type |
|---|---|
| 1 | Sensitive fine grained |
| 2 | Organic material |
| 3 | Clay |
| 4 | Silty clay to clay |
| 5 | Clayey silt to silty clay |
| 6 | Sandy silt to clayey silt |
| 7 | Silty sand to sandy silt |
| 8 | Sand to silty sand |
| 9 | Sand |
| 10 | Gravelly sand to sand |
| 11 | Very stiff fine grained |
| 12 | Sand to clayey sand |

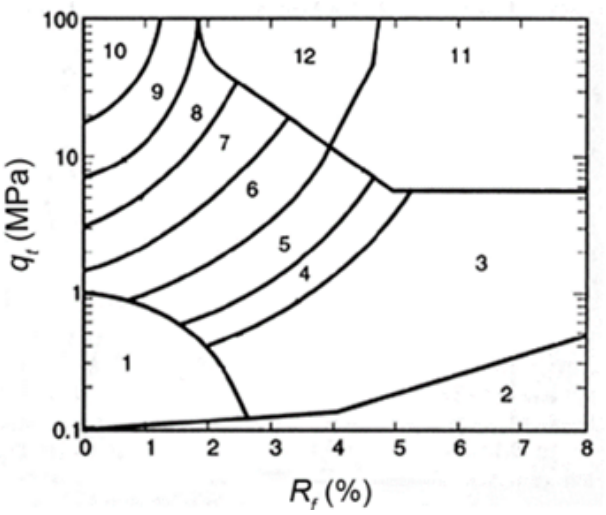


**Figure 1:** Roberson soil behaviour type classification chart[7]

Another very popular classification is the 1990 Robertson classification[11] is presented in Figure 2. It is a further development and improvement of the 1986 method. This classification is based on the normalized cone resistance $Q_{tn}$ and the normalized sleeve friction $F_r$. The number of soil behaviour types has been reduced to 9, as depicted in Table 2. In 2009, Robertson updated the standardized cone resistance and linked it to the SBT diagram.[10]

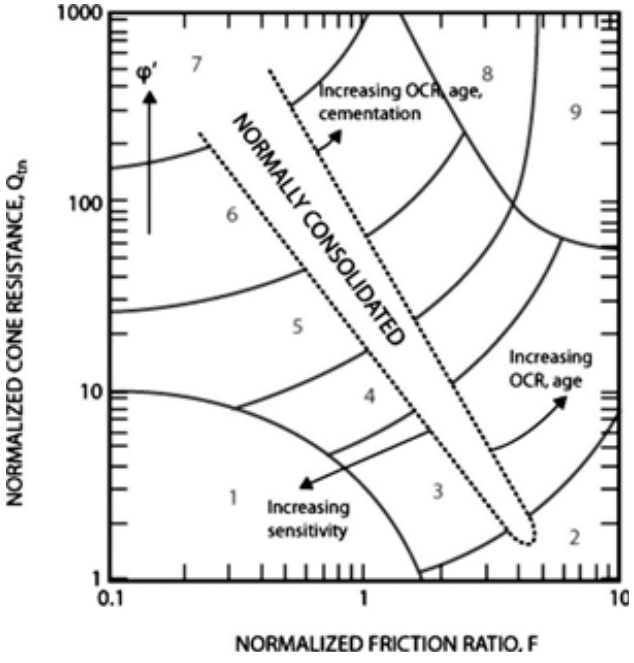


**Figure 2:** Roberson's soil behaviour type classification chart[11]

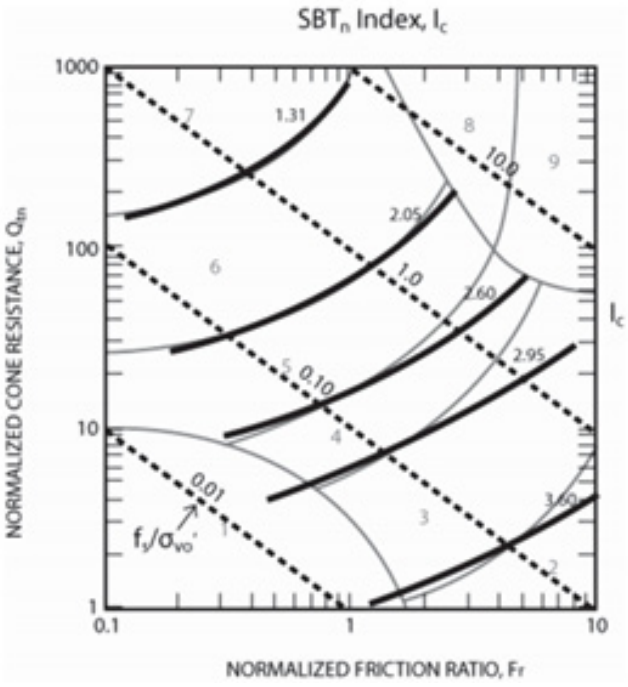


**Figure 3:** The $I_c$ thresholds showed on Roberson's soil behaviour type classification chart[8]

**Table 2:** Numbers of subdivisions and corresponding Soil Behaviour Types[11]

| SBT | Soil behaviour type |
|---|---|
| 1 | Sensitive, fine grained |
| 2 | Organic soils: peats |
| 3 | Clays: silty clay to clay |
| 4 | Silt mixtures: clayey silt to silty clay |
| 5 | Sand mixtures: silty sand to sandy silt |
| 6 | Sand: clean sand to silty sand |
| 7 | Gravelly sand to dense sand |
| 8 | Very stiff sand to clayey sand |
| 9 | Very stiff, fine grained |

It is possible to classify soil layers using the soil behaviour type index $I_c$.[8] By calculating the value of the $I_c$ index, it is possible to determine the soil behaviour type.[9] This method is based on Robertson's classification from 1990[11] but it does not include types from areas 1, 8 and 9. The value of $I_c$ is calculated from formula (6) based on $Q_t$ and $F_r$. The SBT index $I_c$ depends on numerous parameters, however, it is indicated that there is some correlation between the soil grain-size and the value of the $I_c$ index, that is, the higher the index value, the smaller the grain-size.[8] The $I_c$ thresholds are showed on Roberson's soil behaviour type classification chart in Figure 3 and presented in Table 3.

## 1.3 Analysis of the impact of soil layering on the CPTu recordings

Cone Penetration Test provides a wide range of information for estimating soil properties in the profile. However, it should be noticed that the registration at a single point at a given depth is influenced by the spatial arrangement of layers located above and below the cone.[2]

This can be explained by analogy with the pile in the limit state when the failure mechanism pass through the layers above and below the position of the pile base (cone tip).[6][13] Therefore, the measurement characteristics $q_c$ and $f_s$ depend on the order and properties of all soils within the impact zone of the pushed-in cone (Figure 4).

Figure 5 presents the schema of the effect of thin layer and transition zone. On the left side of the picture, five profiles with different capability are shown. On the right side, the cone resistance to depth relation is presented. For the week layer (Profile 1), the resistance under the cone tip is significantly lower than for the strong layer (Profile 2). Lines 3°, 4° and 5° presents the transition between various layers. When the cone is beginning to reach the strong layer, the resistance under the cone tip is smoothly increasing, and respectively, when it is leaving the strong layer, the resistance is smoothly decreasing.

The cone resistance is marked as $q^t$ if the registration would be free from the influence of weaker soil under

**Table 3:** SBT index classification proposed by Robertson and Wride[8]

| Classification | Soil behaviour type | Soil behaviour type index $I_c$ |
|---|---|---|
| SBT2 | Organic soils: peats | $I_c > 3.60$ |
| SBT3 | Clays: silty clay to clay | $2.95 \le I_c < 3.60$ |
| SBT4 | Silt mixtures: clayey silt to silty clay | $2.60 \le I_c < 2.95$ |
| SBT5 | Sand mixtures: silty sand to sandy silt | $2.05 \le I_c < =2.60$ |
| SBT6 | Sand: clean sand to silty sand | $1.31 \le I_c < =2.05$ |
| SBT7 | Gravelly sand to dense sand | $I_c < 1.31$ |

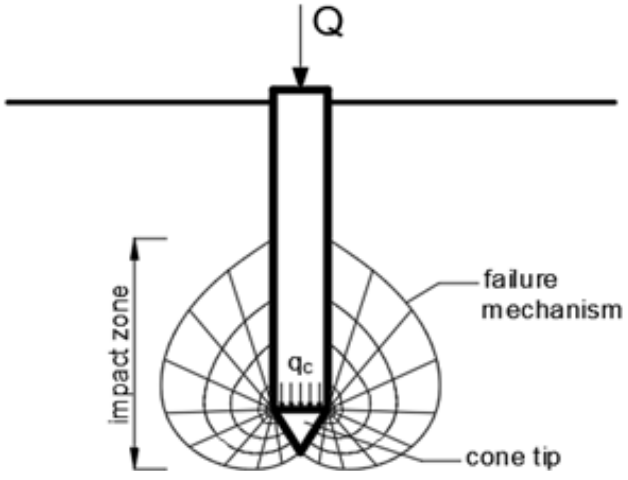


**Figure 4:** Illustration of failure mechanism and impact zone for pile[13]

and above it.[2] Transition zones are defined as interval of depth near the layer boundary where the registration value increases or decreases even though changes rapidly only where the layer boundary occurs. A thin layer effect occurs when the peak $q_c$ is smaller than the corresponding $q^t$. In the cases analyzed in the graphs, the thinner the layer, the difference between the two parameters becomes greater.

The effects related to the soil layering and correct stratification were studied very intensively over the years. In the work by Boulanger R.W. and DeJong J.T.,[2] there is an overview and summary of the achievements to this field. The book[7] contains a solution based on a simplified elastic solution developed by Vreugdenhil.[14] In order to reduce the influence of spatial distribution of layers around the cone on the CPTu sounding records of a certain depth, a correction coefficient of the cone's resistance is applied depending on the thickness and relative stiffness of the layers. The relative stiffness is expressed as the ratio of average resistance of a cone in the layer to registration in the surrounding soil.

A different approach to the stratification problem in CPT measurements is suggested in Boulanger and DeJong.[2] The authors postulate that the cone penetrometer behaves as a low-pass spatial filter and in order to get rid of the influence of adjacent layers, it is necessary to go through the inverse filtration procedure. Low-pass spatial filters are widely used in image and signal processing. A low-pass

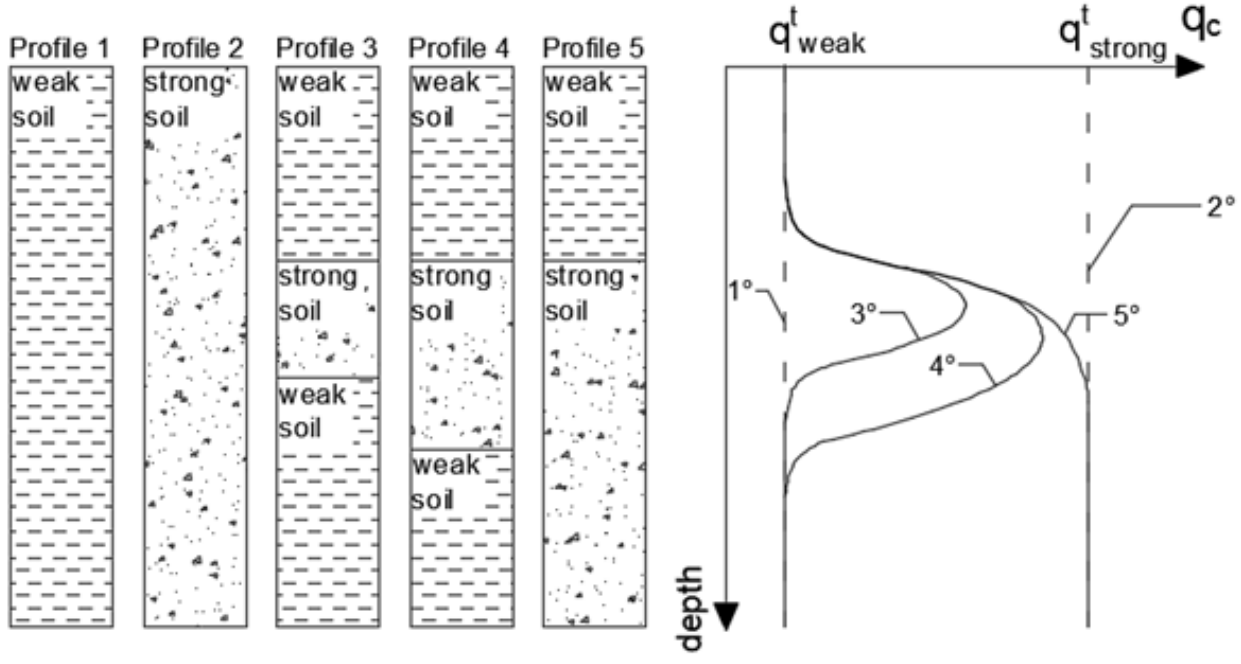


**Figure 5:** The schema of the effect of thin layer and transition zone[2]

spatial filter is also called a fuzzy or smoothing filter. It averages rapid changes in intensity. The simplest low-pass spatial filter calculates the average from a particular pixel using its nearest vicinity. The result obtained from this operation replaces the pixel value. With this procedure, it is possible to smooth the image and blur the contours. Reverse filtering can help restore the value of the image before filtering, if it is possible to develop a function that has blurred the record. In the study stated above, a filter that allows to go through the reverse filtering procedure for CPT probing was developed.

Due to the above mentioned phenomena, that is, the occurrence of the thin layer effect and transition zone, precise detection of the location of layer boundaries is difficult, which often results in errors in recognition of the ground, determination of the layout and thickness of layers in the geological profile, which can further contribute to geotechnical design errors and affect the stability and safety of structures.[12]

The issue related to the separation of layers and the precise determination of their boundaries was dealt with by many researchers. Focciorusso and Uzzielli proposed a procedure of stratification based on cluster analysis and fuzzy algorithm.[4] On the other hand, the Bayesian approach presented by Wang, Huang and Cao[16] is used to separate layers but also allows to determine the probability with which a given soil will qualify for a specific SBT. This approach allows to determine the number of probable layers too. In recent years, the focus has been on the possibility of using machine learning to interpret CPTu sounding. The paper[15] presents a Bayesian unsupervised learning approach allowing to separate layers based on the analysis of parameter variability in two dimensions ($Q_t$, $F_r$).

The authors' paper presents the simple procedure of stratification using high-pass spatial filters, which gives a reasonable result with significantly computational cost in comparison to the mentioned above methods.

## 2 Characterisation of high-pass spatial filters

High-pass spatial filters are a widely used tool in digital signal and image processing.[3] These filters allow obtaining a sharper image or exposing certain image elements. Mathematically, the filtering effect can be presented as a convolution operation of a certain signal $f(x)$ and a high-pass filter $g$(x) the result of which is function $h$(x), according to equation (9).

$$h(x) = (f * g)(x) = \int_{-\infty}^{\infty} f(x-\tau)g(\tau)d\tau \tag{9}$$

Images as well as CPT recordings are considered to be discrete, and therefore, high-pass spatial filtering is considered to be a discrete convolution according to equation (10).

$$h_i = \sum_{k=-\infty}^{\infty} f_{i-k} \cdot g_k \tag{10}$$

These types of filters are commonly used to detect edges in an image.[3] An edge is a rapid change in recording intensity. The graphical interpretation of the perfect edge is shown in

Figure 6a. Edges of this kind are relatively simple to detect because they are located exactly in point $x_0$. Mathematically, they can be described by formula (11).

$$I(x) = \begin{cases} I_1 \; if \; x < x_o \\ I_2 \; if \; x \geq x_o \end{cases} \tag{11}$$

In fact, the change in the intensity of the function never occurs exactly as in Figure 6a. It generally resembles the one in Figure 6b. There is always a certain transition zone (as in the case of CPTu sounding), which may be either linear or non-linear according to equation (12). Using this type of equations, it is difficult to localize an edge because it occurs on a certain length (referring to

Figure 6b., between $x_1$ and $x_2$).

$$I(x) = \begin{cases} I_1 \; if \; x < x_1 \\ f(x) \; if \; x_1 \leq x < x_2 \\ I_2 \; if \; x \geq x_2 \end{cases} \tag{12}$$

One of the elementary high-pass spatial filters allowing for edge detection is the Prewitt's operator.[3][5] It is a discrete differentiation operator that allows to approximate directional signal intensity derivatives. In this kind of filters, it is assumed that the edge occurs in the place where the increase in intensity change is greatest that is equivalent to the maximum gradient. In turn, the maximum gradient usually corresponds to nullifying the second derivative. The directional derivative is determined using the operation of a two-dimensional discrete convolution of the matrix and high-pass filter. When the analysed signal is an image, each cell in the

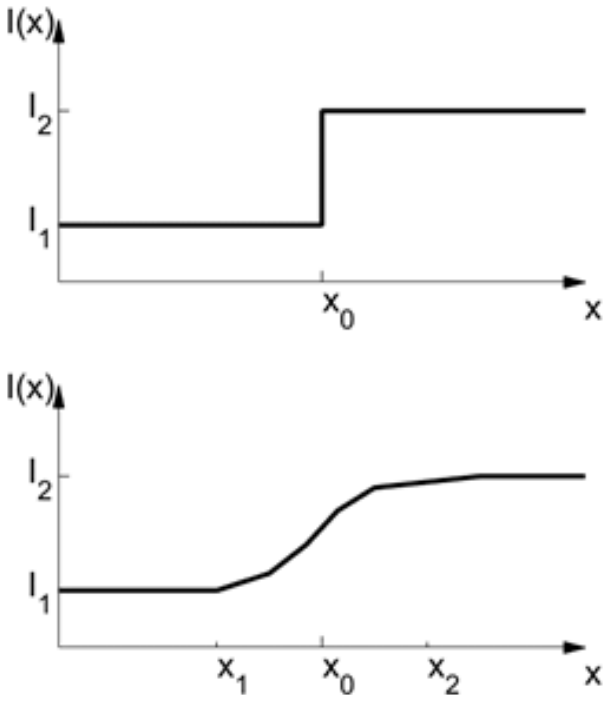


**Figure 6:** Illustration of the edge a) perfect edge, b) blurred edge.

matrix corresponds to a separate pixel. A numerical value is assigned to the corresponding colour, which is then found in this matrix instead of the colour. The filter matrix is a 3x3 square matrix characteristic for a given direction called the transformation kernel (mask). The masks for the horizontal (marked as X) and vertical (marked as Y) directions are different and have the form presented in formula (13).

$$X = \begin{bmatrix} -1 & 0 & 1 \\ -1 & 0 & 1 \\ -1 & 0 & 1 \end{bmatrix} \quad Y = \begin{bmatrix} 1 & 1 & 1 \\ 0 & 0 & 0 \\ -1 & -1 & -1 \end{bmatrix} \tag{13}$$

The final pixel value is calculated according to equation (14) and is given by the sum of the absolute values of the convolution of the image matrix and the high-pass filter in horizontal and vertical direction.

$$h_{i,j} = \left| \sum_{k=1}^{3} \sum_{m=1}^{3} f_{i-2+k,j-2+m} \cdot x_{k,m} \right| + \left| \sum_{k=1}^{3} \sum_{m=1}^{3} f_{i-2+k,j-2+m} \cdot y_{k,m} \right| \tag{14}$$

The Prewitt operator averages the directional derivative from three cells with weights of 1, 1, 1 in the direction parallel to the direction of differentiation according to the masks contained in formula (13). It means that the resulting pixel is scaled from the original matrix by a value of 3. For this reason, in order to keep the same grayscale after and before filtering, the final value in the pixel should be divided by 3.

# 3 Stratification method based on high-pass spatial filters

In order to determine the spatial distribution of layers and assess the type of soil, an original idea of stratification based on a spatial high-pass filter was developed. The calculation procedure is presented below. The basic assumption are:

- Robertson's SBT classification chart and $I_c$ index classification are used,
- normalisation of the parameters is performed according to,
- the Prewitt's operator is applied,
- stratification is based on the normalised cone resistance $Q_{tn}$ and normalise friction ratio $F_r$,
- Wolfram Mathematica software is used.

## 3.1 Step I – calculation of the basic standardized parameters

In the first step, on the basis of the original measurement CPTu sounding values, the standardized parameters should be calculated.

## 3.2 Step II – changing 1D signal into a 2D image

Prewitt's operator described above is used in 2D objects, therefore, it is necessary to extend the dimension of the analysed parameter ($q_c$, $f_s$, $Q_{tn}$, $F_r$) from 1D to 2D by copying the data vector at least twice. $Z \times 1 \rightarrow Z \times 3$, where $Z$ – number of records in the probe. This procedure is executed for each normalized parameter individually. Each generated array is then normalised by dividing by a maximum value. In this way, the values in the array are in the range of 0 to 1. The last step is to assign a colour value such that the maximum value is white, the minimum value is black, and the intermediate values have grayscale shades. As the values of the parameters in the rows have the same values, they are represented by horizontal monochromatic stripes consisting only of grayscale shades.

### 3.3 Step III – high-pass filtering of the recording image

The following step is to apply a high-pass spatial filter to the image from the Step II. The algorithm uses the Prewitt operator.[3][5] Due to the lack of variability of parameters in the horizontal direction in the signal matrix resulting from the extension of the 1D to 2D image by copying their values, a horizontal task dimension greater than 3 does not affect the solution because the directional derivative in the horizontal direction is always zero. As a result of applying a filter, a matrix where value 1 correspond to the occurrence of an edge and 0 to its absence is obtained.

### 3.4 Step IV – defining the strata boundary according to detected edges

In case of a classification based directly on the classification index $I_c$,[9] the detected edges in the image may be immediately taken as the boundary of layers in the geological profile because this classification is based only on one parameter. In a classification based on Robertson's nomogram,[10] the situation is complicated because it is based on two standardised values ($Q_{tn}$ and $F_r$). In the images of registration after using Prewitt's operator, the edges are not always detected at the same depth for both parameters. In addition, due to the geometric structure of the cone, the resistance records on the friction sleeve is a few cm above the resistance measurement level under the cone tip, the maximum offset of the detected edges can be up to 10 cm. The algorithm first searches for the edge at $Q_{tn}$ image and then verifies if the edge is also detected at $F_r$ in the vicinity depth. If an edge occurs in this area, the edge in the image is identified with the border of layers in the geological profile; if not, the detected edges are not identical with the borders of layers in the geological profile.

### 3.5 Step V – calculation of the average parameter values within the layer

After determining the strata boundary in the geological profile from the registration images, it is possible to return to the original standardized registrations. The process of evaluating the representative parameters within the separated layers is based on calculating the average value of each standardized parameter, taking into account the fact that transition zones exist near the layer boundaries.[2] The fact of the occurrence of disturbances at the strata' borders is taken into account by rejecting the values located within 7 cm (approximately two diameters of the cone) from the boundary of the layer from the set taken into account for counting the average. The value of 7 cm was taken as the minimum thickness of the impact zone, for which the measurement results are most disturbed.[2]

### 3.6 Step VI – soil behaviour type classification

In further operation, the classification should be made on the assumption of representative parameters; firstly based on $Q_{tn}$ and $F_r$ for the 1990 Robertson classification[10] and next based on $I_c$ for the classification based on the classification coefficient.[9]

### 3.7 Step VII – comparison of both classifications

The final stage of the stratification procedure is to compare the results obtained for different classifications. If a point is classified into the same group of SBTs according to different classifications, it is more likely that the classification of the strata into a given group is correct.

## 4 Results

The algorithm presented previously was implemented to solve a competition task in accordance with TC304 Student Contest on Spatial Data Analysis. The organizers of this contest provided the CPTu soundings results in the form of one training dataset and three tests datasets. The training dataset varied from the others in the fact that it was accompanied by a rational stratification carried out by professionals in order to compare it with the results obtained using the algorithm.

The results of the analysis are shown in Figure 7 to Figure 10. The subheadings are presented consecutively: a) image of registration $q_t$; b) image of registration $f_s$; c) edges detected by using the high-pass filter presented above; d), e), f), g) registration graphs of $q_t$, $f_s$, $Q_{tn}$ and $F_r$ respectively, together with average values in layers; h) soil type classification carried out according to Robertson nomogram based on $Q_{tn}/F_r$ for each point individually and for parameters averaged in layer; i) a graph of the classification index values $I_c$ for each point individually and for parameters averaged over the layer; j) the soil type

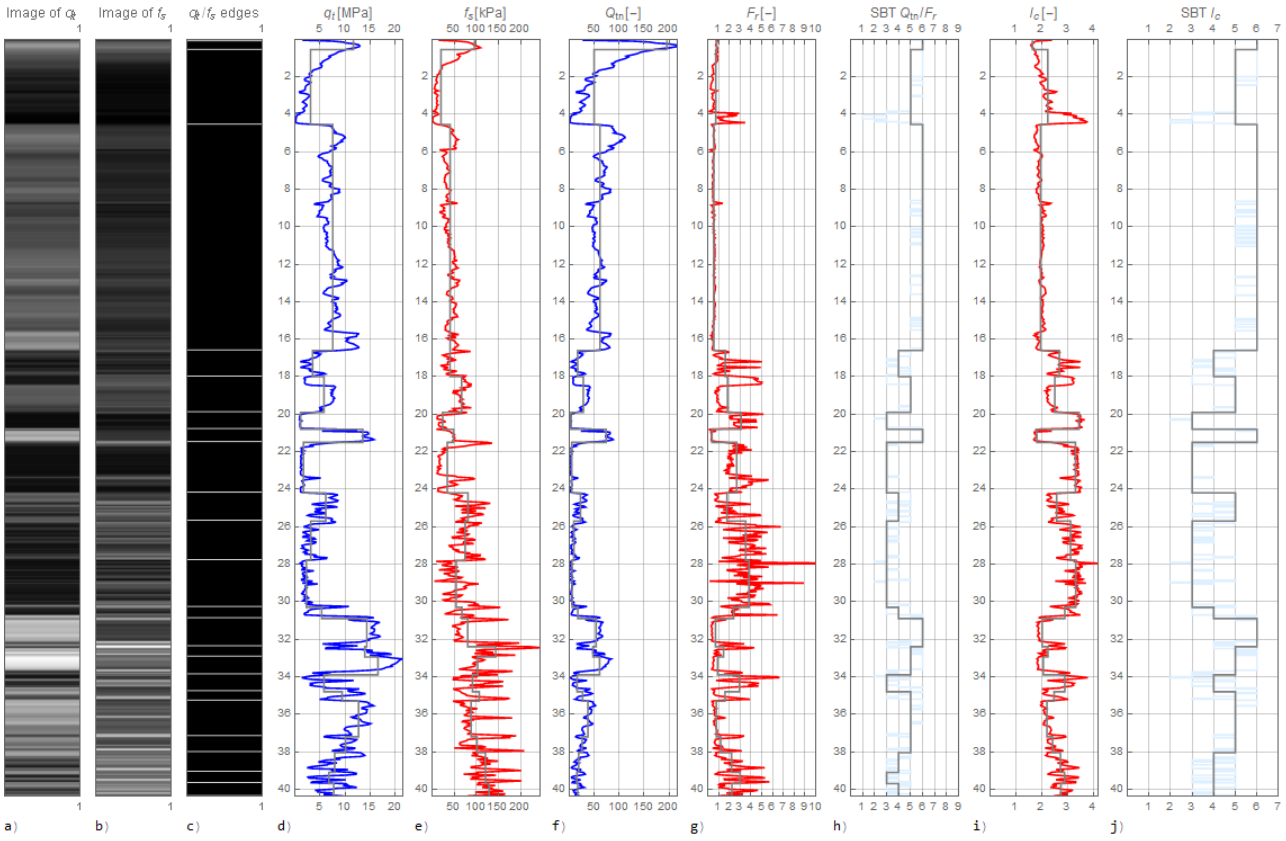


**Figure 7:** Results obtained with algorithm on training dataset.

classification based on the classification index $I_c$ for each point individually and for parameters averaged over the layer.

## 5 Discussion of results

The algorithm presented in section 3, despite its high level of automation, requires control of the obtained results. It detects the strata boundary of high-contrast layers, which is clearly visible in Figure 8. Soils with parameters changing in a smooth way, with a clear trend but without value jumps may become problematic. Such soils are, for example, dumpling soils,[1] which are in the scope of the authors' research and future development plans to examine the possibility of using this algorithm for their analysis. The use of different classifications may result in the detection of layer boundaries at different locations. The authors used the Robertson classification[11] as a reference classification. It is possible that an edge detected by analysing the variability of the sounding chart will not divide a particular layer into two due to the fact that the SBT classification is in the same order.

## 6 Conclusions

After analysing the results obtained from the stratification carried out using high-pass spatial filters, it can be concluded that it produces rational solutions. By separating the strata boundaries and then averaging the values inside the strata, the measurement becomes significantly insensitive to noise, which in case of separation of the strata in the ground profile is identified with a large number of very thin layers. In addition, in Figure 7 to Figure 10, it is possible to observe that the averaged parameters correspond closely to the actual soundings. The Organizers of the competition TC304 Student Contest on Spatial Data Analysis (September 22, 2019, Hannover, Germany) provided the test data set in the form of CPTu sounding and stratification carried out using proven methods and experts' knowledge. The proposed algorithm was supposed to provide the best possible entry into the proposed stratification.

Figure 11 depicts a comparison of the results provided by the organisers of the competition with the results obtained using the algorithm. As it may be noticed, the stratification carried out through the algorithm seems to

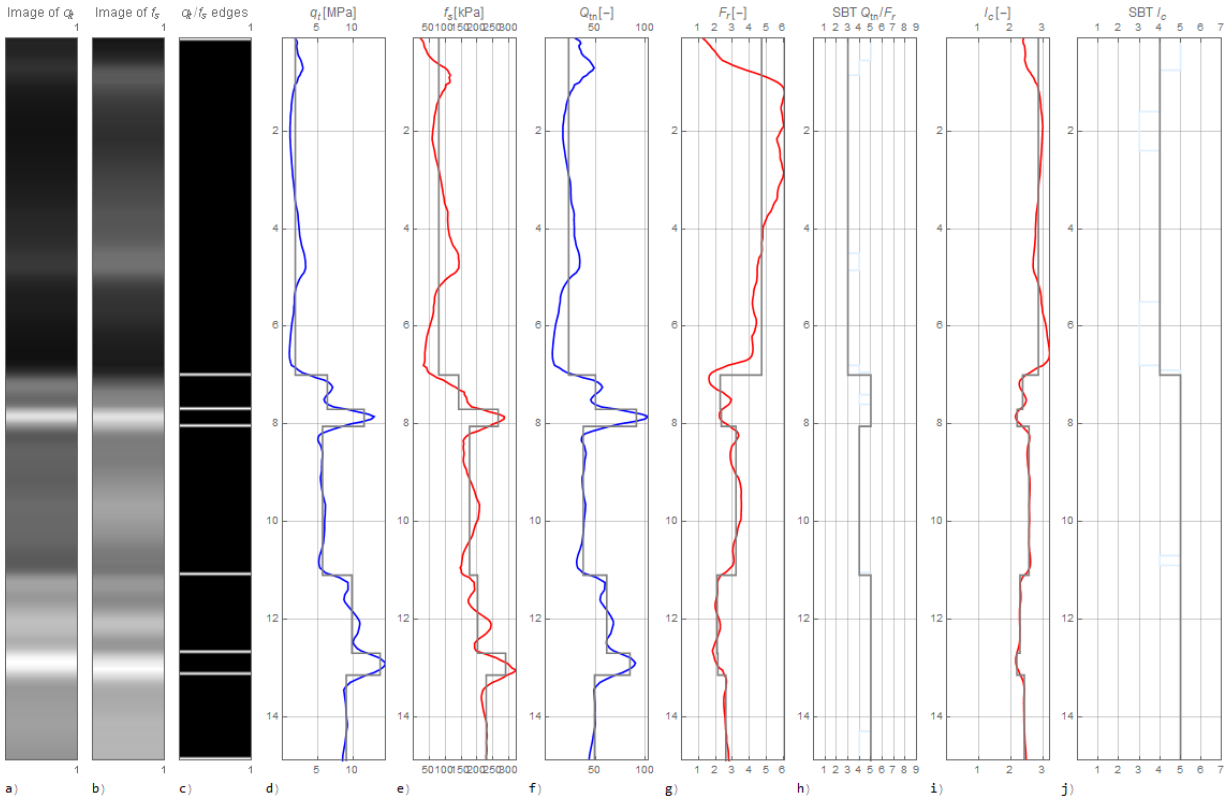


**Figure 8:** Results obtained with algorithm on testing dataset 1.

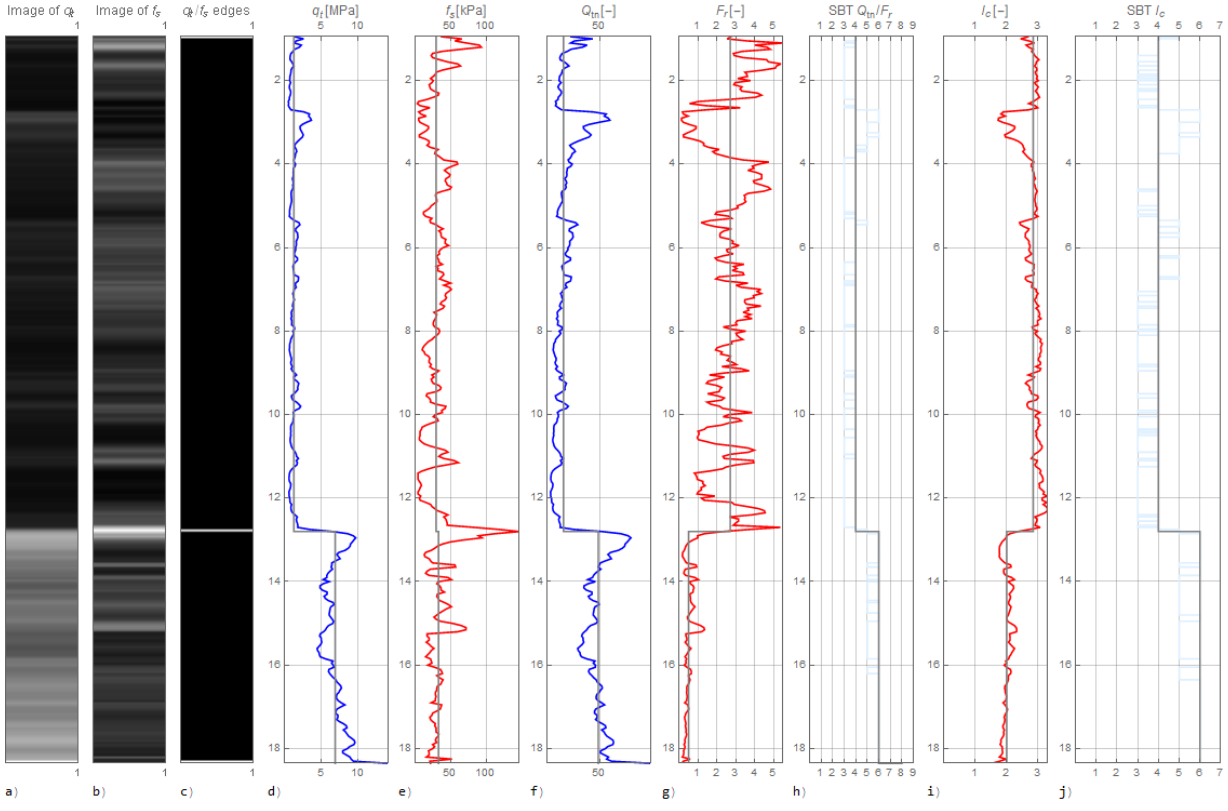


**Figure 9:** Results obtained with algorithm on testing dataset 2.

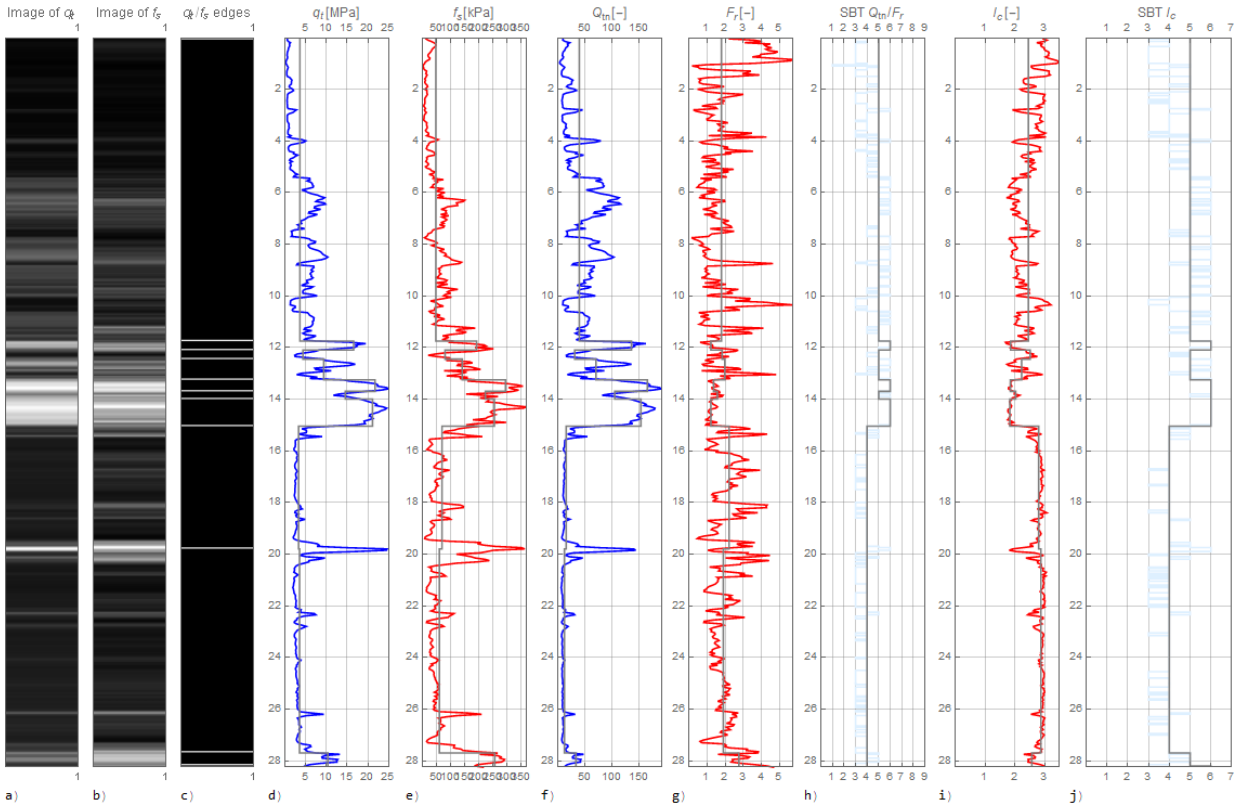


**Figure 10:** Results obtained with algorithm on testing dataset 3.

be reasonable and leads to a stratification that is similar to expert analysis. Separated strata boundaries occur at highly similar depths. Additionally, in most cases, the classification according to Organizers and authors is consistent. On this basis, it is possible to deduce that the algorithm works in a proper way.

The quality assessment of the degree-of-belief of stratification is a task that required the knowledge about exact strata boundaries locations in the ground. The qualitative analysis of the proposed algorithm in comparison to the different boreholes' tests remains the subject of a future research work of the paper authors.

The novelty of the stratification method comes from the application of tools not previously used in this area, in the form of high-pass spatial filters, which were primarily used in digital image processing. The results of the analysis confirm the observation that CPTu registrations may be considered as a signal and there is nothing to prevent the possibility of employing similar tools for their processing.

A possible area to implement the algorithm described above may be the analysis of the spatial variability of dumping grounds, where additionally, there is a need to create a completely new classification, so this tool may be used for preliminary selection of layers with similar characteristics.

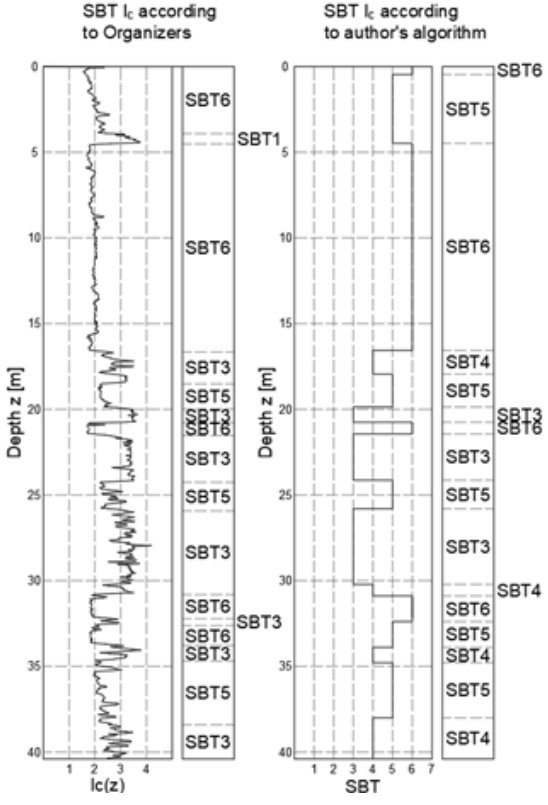


**Figure 11:** Comparison of stratification according to Organizers and authors.

**Acknowledgements:** We would like to thank Prof. CS Ku in I-Shou from University Taiwan, for providing the CPTu data.

## References

[1] Bagińska I., Kawa M., Janecki W.: Estimation of spatial variability of lignite mine dumping ground soil properties using CPTu results, Studia Geotechnica et Mechanica 38(1), pp. 3–13, 2016
[2] Boulanger R.W., DeJong J.T.: Inverse filtering procedure to correct cone penetration data for thin-layer and transition effects, Cone penetration testing 2018: procedding of the 4th International Symposium on Cone Penetration Testing, pp. 25–44, 2018
[3] Cristobal G., Schelkens P., Thienpont H.: Optical and Digital Image Processing: Fundamentals and Applications, Wiley- VCH Verlag GmbH&Co. KGaA, 2011
[4] Facciorusso J., Uzzielli M., Stratigraphic profiling by cluster analysis and fuzzy soil classification, Proceedings of the 2nd International Conference on Geotechnical Site Characterization ISC-2, Porto, 2004
[5] Kowalski P., Czyżak M., Smyk R.: Comparison of edge detection algorithms for electric wire recognition, ITM Web of Conferences 19, 01044, 2018
[6] Lim Yi Xian, Numerical study of cone penetration test in clays using press-replace method, National University of Singapore, 2017
[7] Lunne T., Robertson P.K., Powell J.J.M.: Cone penetration testing in geotechnical practice, Blackie Academic, EF SPON/ Routledge Publishing, 1997
[8] Roberson P.K. Wride C.E. Evaluating cyclic liquefaction potential using the cone penetration test, Canadian Geotechnical Journal, pp. 442–459, 1998
[9] Robertson P.K.: Cone penetration test (CPT) – based soil behaviour type (SBT) classification system- an update. Canadian Geotechnical Journal, pp. 1910–1927, 2016
[10] Robertson P.K.: Interpretation of cone penetration test – a unified approach, Canadian Geotechnical Journal 46(11), pp. 1337–1355, 2009
[11] Robertson P.K.: Soil classification using the cone penetration test, Canadian Geotechnical Journal 27(1), pp. 151–159, 1990
[12] Rybak J., Stilger-Szydło E.: Importance and errors in the identification of the ground in the foundation of land transport infrastructure structures (in Polish), Nowoczesne Budownictwo Inżynieryjne 4, pp. 60–65, 2010
[13] Van Baars, S.: 100 Years of Prandtl's Wedge, Amsterdam: IOS Press, Incorporated, 2018
[14] Vreugdenhil R., Davis R., Berrill J.: Interpretation of cone penetration results in multi-layered soils, International Journal for Numerical and Analytical Methods in Geomechanics, vol. 18, 585–599, 1994
[15] Wang H, Wang X., Wellmann F, Liang R., A Bayesian unsupervised learning approach for identifying soil stratification using cone penetration data. Canadian Geotechnical Journal, 2018
[16] Wang Y., Huang K., Cao Z., Probabilistic identification of underground soil stratification using cone penetrations test, Canadian Geotechnical Journal, pp. 766–776, 2013